Numerical Generation of Multidimensional Flamelet Databases using an Adaptive Wavelet Method

S. Gemini[a,*], P. P. Ciottoli[a], R. Malpica Galassi[a], T. Grenga[b], H. Pitsch[b], S. Paolucci[c], M. Valorani[a]

[a]Department of Aerospace and Mechanical Engineering, University of Rome "La Sapienza", Rome, RM 00184, Italy
[b]Institute for Combustion Technology, RWTH Aachen University, Aachen 52056, Germany
[c]Aerospace & Mechanical Engineering, University of Notre Dame, Notre Dame, IN 46556, USA

Abstract

The Wavelet Adaptive Multiresolution Representation (WAMR) code is used for the numerical time integration of the one-dimensional laminar diffusion flames equations in trans-critical and supercritical conditions, where the thermodynamic and transport properties exhibit large changes. These steep gradients are efficiently captured by the WAMR algorithm with an a-priori defined accuracy and an associated large reduction of the number of degrees of freedom, allowing a highly efficient flamelet database generation for flows which usually operate under supercritical and near-critical conditions.

Keywords: Flamelet, Wavelet, Supercritical

Introduction

The requirement of high performance in liquid rockets and diesel engine combustion can be achieved by increasing the pressure in the combustion chamber. This could lead to the injection of oxidizer and/or fuel at pressure and temperature values exceeding the critical point. Beyond this point the fluid is in supercritical thermodynamic conditions. In trans-critical and near-critical conditions the thermodynamic and transport properties are characterized by abrupt variations.

In this context a study of the one-dimensional laminar diffusion flames for non-premixed combustion at high pressure conditions is proposed. Their behaviour have been deeply invetigated by Kim et al. [1, 2] using a direct approach, where the solution is given in the mixture fraction space. By following this approach, they performed steady-state analysis for kerosene/LOx rocket combustion [1] and hydrogen/liquid oxygen [2] in supercritical states. Unsteady effects of non-premixed methane/oxygen flame structures at supercritical pressures have been instead explored by Lapenna et al. [3], choosing an arbitrary non-uniform grid suitably compressed towards the oxidizer side, where higher resolution is required to capture the steep gradients characterizing the solution. The main purpose of the current work is to overcome this limitation, by using a wavelet-based collocation method to build a dynamically adaptive grid using a mathematical method for the selection of the grid points that ensures an a-priori prescribed accuracy.

* Corresponding author: simone.gemini@uniroma1.it
Proceedings of the European Combustion Meeting 2019

The Wavelet Adaptive Multiresolution Representation (WAMR) code [4, 5] is the framework used in this work to generate steady-state solutions of one-dimensional flamelet equations. This method has been implemented by Grenga [6] for massive parallel application on high performance computing and it was also verified [5, 7] for a wide range of test cases - compressible and incompressible flows described by reacting Navier-Stokes equations in primitive variables in 1-, 2- and 3-D geometries. WAMR is particularly suited for the solution of multidimensional continuum physics problems having a strong multiscale character. It generates a dynamically adaptive grid able to capture any desired accuracy, and produces an automatically verified solution. In addition, the efficient implementation minimizes the memory footprint and the computing time, reducing the required computational resources.

Using the WAMR algorithm to determine the dynamically adaptive grid for the flamelet problem, the computational cost is expected to be largely reduced: steep gradients are well captured by the algorithm, with a relative reduced number of grid points and a consequent extreme reduction of the computational cost. Therefore, accurate chemical kinetic mechanisms involving a large number of chemical species and reactions can be used to solve flamelet problems. Furthermore, more complex and expensive Equations of State (EoS) can be adopted to better describe the fluid behaviour in non-ideal conditions.

These features allow the generation of multidimensional flamelet databases for high-pressure combustion devices which usually operate under supercritical con-

ditions. Small size databases will be obtained through the WAMR algorithm. It will optimize the tables along multiple directions, like for example mixture fraction, pressure and scalar dissipation rate.

The wavelet representation

In this context, a dyadic structure of the grid is used to build adaptive grids through the wavelet-based collocation method. Following this methodology, the function values can be reconstructed as the sum of wavelet functions, where their amplitudes represent the difference between the actual value of the function and the one obtained through wavelet interpolation at the corresponding resolution level. This difference represents the local error; it decreases increasing the wavelet interpolation order and/or increasing the number of refinement levels because of a better reconstruction of the function value is obtained. The adaptive grid is built looking at the values of the wavelet amplitudes: if they are lower than an a-priori user-prescribed threshold parameter ε the grid point is simply removed, otherwise it becomes a point requested for the wavelet representation, namely an essential point. The final grid will be only composed by essential, neighbouring and non-essential points: the solution is advanced only on the essential and neighbouring points, while the non-essential points are included to complete stencils needed in various operations on the sparse grid. Complete details about the grid constructions can be found in the work of Grenga [6] and Wirasaet [8].

The flamelet model

The unsteady flamelet equations taken by Pitsch and Peters [9] are considered for adiabatic case, at constant pressure and unity Lewis number,

$$\frac{\partial Y_i}{\partial t} = \frac{\chi}{2}\frac{\partial^2 Y_i}{\partial z^2} + \frac{\dot{\omega}_i}{\rho} \qquad i = 1, \ldots, N_s \quad (1)$$

$$\frac{\partial T}{\partial t} = \frac{\chi}{2}\frac{1}{c_p}\frac{\partial^2 h}{\partial z^2} - \frac{\chi}{2}\frac{1}{c_p}\sum_{k=1}^{N_s} h_k \frac{\partial^2 Y_k}{\partial z^2} - \frac{1}{\rho c_p}\dot{\omega}_T \quad (2)$$

where t is the time, Y_i represents the mass fractions of the i-th species, χ is the scalar dissipation rate, z is the mixture fraction variable, $\dot{\omega}_i$ is the production rate for the i-th species due to chimical reactions, ρ is the density, T is the temperature, c_p is the specific heat at constant pressure, h is the enthalpy of the mixture, N_s is the total number of mixture components, h_k is the enthalpy of the k-th species, and $\dot{\omega}_T = \sum_{k=1}^{N_s} h_k \dot{\omega}_k$ is the rate of enthalpy production due to the variation in the composition of the mixture. The scalar dissipation rate is expressed as a function of the mixture fraction as shown by Girimaji [10], $\chi = \chi^0_{max}\exp(-2\mathrm{erfc}^{-1}(2z))^2$.

The flamelet equations are solved considering the CH_4/O_2 RAM accelerator kinetic mechanism (RAMEC) Petersen et al. [11], taking into account 38 chemical species and 190 reactions.

Real gas equation of state

In this work the three-parameters Redlich-Kwong/Peng-Robinson (RK-PR) [12] EoS is used to evaluate the thermodynamic properties of the fluid: this choice allows to have an accurate representation of the real fluid properties in an efficient way [1].

It takes the form

$$p = \frac{\rho R_u T}{M_w - b\rho} - \frac{a\alpha(T)\rho^2}{(M_w + \delta_1 b\rho)(M_w + \delta_2 b\rho)}. \quad (3)$$

where p is the pressure, R_u is the universal gas constant and M_w is the molecular weight. Through the parameters a and b the effects of the attractive and repulsive van der Waals forces are considered in the model, respectively; these parameters are functions of the thermodynamic variables at critical conditions (temperature and pressure, T_c and p_c) and of the third parameter δ_1. They can be found also in the two-parameter cubic SRK (Soave-Redlick-Kwong) EoS and PR (Peng-Robinson) EoS, where δ_1 is instead an assigned costant. The additional degree of freedom of RK-PR Eos introduced by [12], δ_1, (note that $\delta_2 = f(\delta_1)$) leads to a better description of the fluid behaviour in terms of density, with respect to the two-parameter cubic SRK EoS and PR EoS usually used. Finally, $\alpha(T)$ is a temperature correction factor taking into account the polarity of the species, it depends on the reduced temperature (defined as T/T_c) and an acentric factor. Exhaustive description of RK-PR Eos including the definitions of all parameters can be found in Cismondi et al. [12].

For a multi-components mixture the RK-PR EoS (3) is defined using conventional mixing rules, details are accuratively described in Kim et al. [1, 2].

Validation of the thermodynamic properties

The thermodynamic properties based on the RK-PR EoS are here compared to the data taken from the National Institute of Standard and Technology (NIST) database [13], considering a pure methane compound, whose critical temperature is $T_{c,CH_4} = 190.564$ K. Figures 1-2 show the values of ρ and c_p for different values of the pressure, in the temperature range $100-400$ K: for

$T \geq T_c$ the fluid is in supercritical conditions. The continuous lines, representing the simulations results, are in good agreement with the reference data, represented by the dots, even if slight errors are present in the zone where there is a transition from subcritical to supercritical conditions. These inaccuracies are attributed to the limitations of the RK-PR EoS, although it provides a more accurate modelling of the density in comparison with the two-parameter EoS. Comparison data for the two-parameter EoS are provided in the study of Kim et al. [1] for saturated hydrocarbons with varying carbon number: the SRK EoS seems to well predict the density for species having a higher critical compressibility factor, instead the PR EoS works better for the larger hydrocarbons characterized by lower critical compressibility factors.

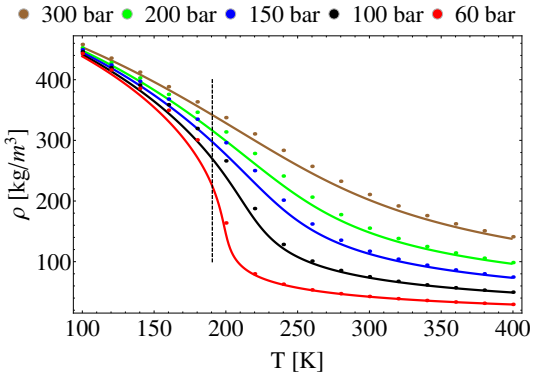

Figure 1: Density at different pressure and temperature values; the dots represent the NIST data, while the continuous lines are the values from RK-PR EoS; the dashed line represents the critical temperature for methane, T_{c,CH_4} = 190.564 K.

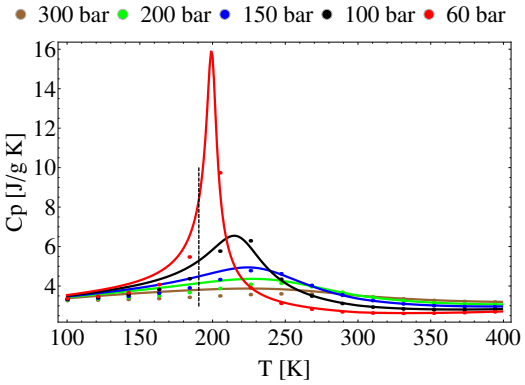

Figure 2: c_p at different pressure and temperature values; the dots represent the NIST data, while the lines are the values from RK-PR EoS; the dashed line represents the methane critical temperature for methane, T_{c,CH_4} = 190.564 K.

Results and discussion

The flamelet equations are initially integrated for p = 60 bar and χ^0_{max} = 200 s^{-1}, choosing $\varepsilon = 10^{-3}$ and sixth-order wavelet functions. The critical pressures and temperatures are p_{c,CH_4} = 45.992 bar and T_{c,CH_4} = 190.564 K for the methane, p_{c,O_2} = 50.430 bar and T_{c,O_2} = 154.581 K for the oxygen [13]. The oxygen and methane are injected at temperatures equal to $T^{in}_{O_2}$ = 120 K and $T^{in}_{CH_4}$ = 1346 K, so they are in liquid-like state and supercritical state, respectively.

The time integration of the flamelet equations is performed through DVODE and the steady-state is supposed to be reached when the root mean square (RMS) of the equations right hand side (RHS) becomes lower than a fixed prescribed minimum value. The steady-state solution is represented in Fig. 3 in terms of temperature: the number of grid points, at the chosen space accuracy, is 80.

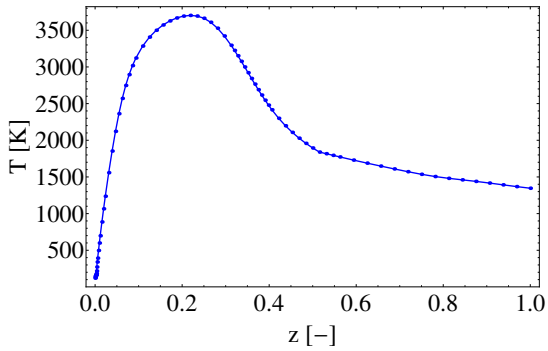

Figure 3: Steady-state solution - temperature for a wavelet threshold parameter $\varepsilon = 10^{-3}$.

A tool to show the efficiency of the wavelet compression is represented by the compression degree π defined as the ratio between the number of grid points of the adaptive mesh and a reference uniform grid having the same minimal spacing. In the current test, the compression ratio is equal to $\pi \simeq 98\%$. A large grid points concentration is present in the vicinity of $z = 0$, where the maximum reached resolution level is $L = 8$: here strong variations of the c_p are present, as shown in Figs. 4-5. This result highlights the excellent capability of the wavelet method to well capture strong variations of the variables, adding grid points at higher resolution levels to ensure the achievement of the prescribed accuracy.

The computational cost associated with the evaluation of the thermodynamic properties in near-critical

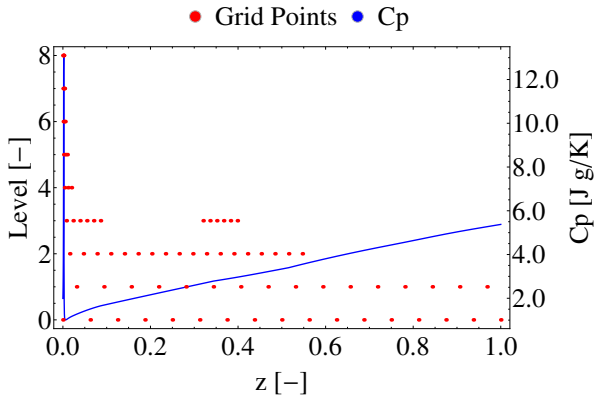

Figure 4: c_p and grid points at different resolution levels; the wavelet threshold parameter is $\varepsilon = 10^{-3}$.

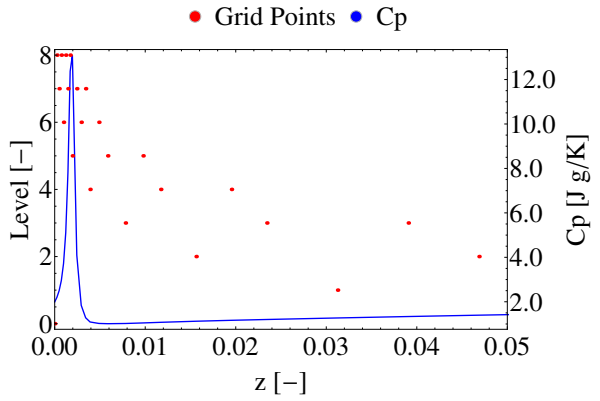

Figure 5: c_p and grid points at different resolution levels for $z = 0 - 0.05$; the wavelet threshold parameter is $\varepsilon = 10^{-3}$.

and supercritical state according with RK-PR EoS represents approximatively the 95 % of the requested time to compute the RHS of Eqs. 1-2. The result can be justified by the highly expensive combination rules adopted to evaluate the thermodynamic properties through the RK-PR EoS for a multi-component mixture. Because of the RHS has to be evaluated in each point of the grid, the use of an adaptive grid allows to reduce substantially the total computational time needed to reach the steady-state.

Table 1 summarizes the results of different simulations, for $p = 60$ bar, $\chi^0_{max} = 200$ s^{-1} and ε varying from 10^{-2} to 10^{-4}: a decrease of the threshold parameters corresponds to an upward trend of the number of grid points N_p, L and π. Indeed, higher resolution levels have to be added in order to obtain more accurate representations of the solution. In particular, Fig. 6 shows how the solution representation changes in the three cases looking at the temperature in the vicinity of $z = 0$, where the maximum resolution level is typically reached because of the extreme variations of the c_p. Figure 6 shows clearly that using $\varepsilon = 10^{-2}$ the wavelet-based algorithm will capture only the temperature trend in the range $z = 0 - 5 \times 10^{-3}$; conversely, in the cases with $\varepsilon = 10^{-3}$ and $\varepsilon = 10^{-4}$ WAMR automatically refines the grid, the triangular symbols represent the added points, capturing also the relatively small temperature variations.

ε	L	N_p	π
10^{-2}	2	35	$\simeq 54\%$
10^{-3}	8	80	$\simeq 98\%$
10^{-4}	11	114	$\simeq 99\%$

Table 1: Maximum resolution level, number of grid points and compression ratio with respect to the threshold parameters, with $p = 60$ bar and $\chi^0_{max} = 200$ s^{-1}.

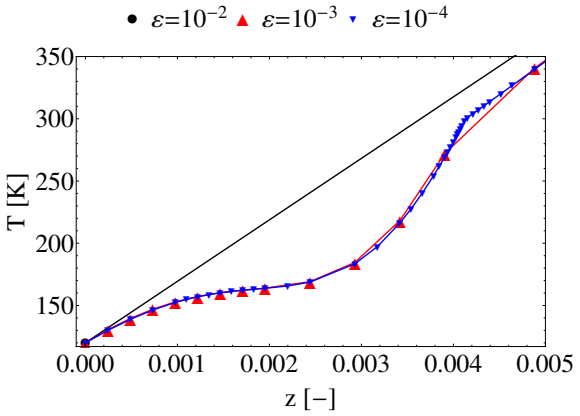

Figure 6: Temperature with respect to the mixture fraction for three threshold parameters, with $p = 60$ bar, $\chi^0_{max} = 200$ s^{-1}.

The pressure effects on steady-state solutions have been investigated in the range $p = 60 - 160$ bar, with $\chi^0_{max} = 100$ s^{-1}. Sixth order wavelet functions and a threshold equal to $\varepsilon = 10^{-3}$ are again used for the wavelet representation. By increasing the pressure, an upward trend for maximum temperature and CO concentration can be observed in Figs. 7-8. Table 2 shows the variation of the maximum resolution with respect to pressure: higher values of the compression ratio are reached for $p = 60$ bar. This is due to a localized-high temperature variation in the vicinity of $z = 0$, that the wavelet-based method is able to accurately capture: the largest number of grid points is concentrated near $z = 0$.

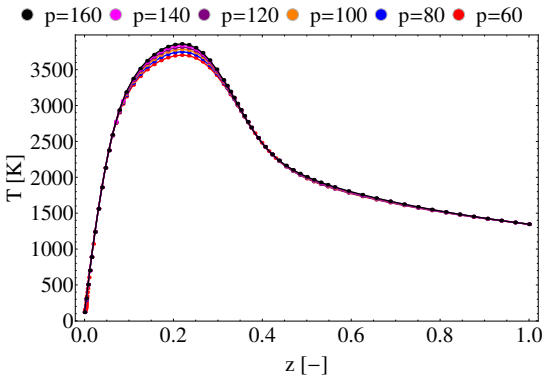

Figure 7: Temperature with respect to the mixture fraction in the pressure range $p = 60 - 160$ bar, with $\chi^0_{max} = 200$ s^{-1}; the threshold parameter is $\varepsilon = 10^{-3}$ and the wavelet order is 6.

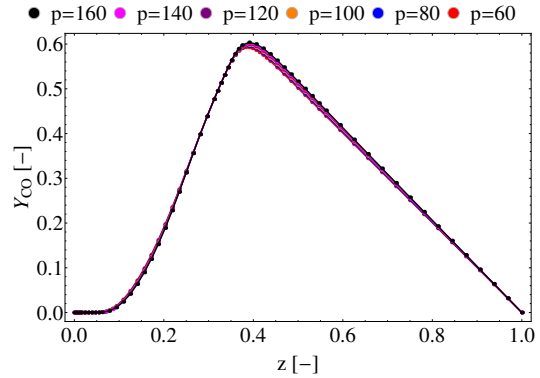

Figure 8: Y_{CO} with respect to the mixture fraction in the pressure range $p = 60 - 160$ bar, with $\chi^0_{max} = 200$ s^{-1}; the threshold parameter is $\varepsilon = 10^{-3}$ and the wavelet order is 6.

p (bar)	L	N_p	π
60	8	80	$\simeq 98\%$
80	4	63	$\simeq 68\%$
100	4	63	$\simeq 68\%$
120	4	63	$\simeq 68\%$
140	4	63	$\simeq 68\%$
160	4	61	$\simeq 68\%$

Table 2: Maximum resolution level, number of grid points and compression ratio with respect to pressure.

Conclusions and future work

The WAMR framework has been used to generate steady-state solutions of the flamelet equations in near-critical and supercritical conditions, using the RAMEC kinetic mechanism. To well describe the fluid behaviour at these conditions, the three-parameters RK-PR EoS has been adopted. The features of the method and the main achievements can be summarized as:

- The density and c_p of the methane at different pressures and temperatures have been evaluated through the RK-PR EoS. These results are in good agreement with reference data.

- By fixing the pressure ($p = 60$ bar), the scalar dissipation rate ($\chi^0_{max} = 200$ s^{-1}) and the threshold parameter ($\varepsilon = 10^{-3}$), the capability of the wavelet method to well capture strong variations of the solutions has been shown: grid points are added only where higher resolution levels are required to ensure the achievement of the prescribed accuracy. The excellent capability of the wavelet compression with respect to a reference uniform grid having the same minimal spacing has been shown evaluating the compression degree, equal to $\pi = 98\%$.

- The evaluation of the thermodynamic properties at grid points in near-critical and supercritical conditions is particularly expensive. The associated computational time represents the 95% of the total computational time requested for the RHS evaluation at each grid point. By using dynamically adaptive grids the number of DOFs is extremely reduce with respect to a reference uniform grid having the same minimal spacing. As a result, the time integration of the flamelet equations results much less expensive.

- By increasing the values of the threshold parameters from $\varepsilon = 10^{-2}$ to $\varepsilon = 10^{-4}$, higher refinement levels are reached, more grid points are added and the compression ratios are larger. Furthermore, smaller solution variations are well captured with smaller threshold parameters.

- Finally, the pressure effects on steady-state solutions have been investigated, fixing $\varepsilon = 10^{-3}$, $\chi^0_{max} = 100$ s^{-1} and varying the pressure from $p = 60 - 160$ bar. Higher resolution levels are only reached in the vicinity of the critical conditions of the mixture, i.e. where the c_p variations are larger.

- This work represents the first step to build the multidimensional tabulated flamelets through the use of the wavelet-based collocation method. They will be obtained through the simulation at different conditions (e.g., pressure and scalar dissipation rate). The wavelet method will be also used

to determine if it is necessary to perform the simulation for given p and χ^0_{max} in order to obtain a multi-dimensional table with the defined accuracy. Preliminary results have been just obtained for the range $p = 60 - 160$ bar and $\chi^0_{max} = 100 - 4000$ s^{-1}.

Acknowledgements

The present work has been supported by the Italian Ministry of Education, University and Research (MIUR) and the Institute for Combustion Technology (RWTH Aachen University).

Funding from of the European Research Council (ERC) under the European Unions Horizon 2020 research and innovation program under grant agreement No 695747 is acknowledged.

References

[1] S.-K. Kim, H.-S. Choi, Y. Kim, Thermodynamic modeling based on a generalized cubic equation of state for kerosene/LOx rocket combustion, Combustion and Flame 159 (3) (2012) 1351 – 1365.

[2] T. Kim, Y. Kim, S.-K. Kim, Numerical analysis of gaseous hydrogen/liquid oxygen flamelet at supercritical pressures, International Journal of Hydrogen Energy 36 (10) (2011) 6303 – 6316.

[3] P. E. Lapenna, P. P. Ciottoli, F. Creta, Unsteady non-premixed methane/oxygen flame structures at supercritical pressures, Combustion Science and Technology 189 (12) (2017) 2056–2082.

[4] S. Paolucci, Z. J. Zikoski, D. Wirasaet, WAMR: An adaptive wavelet method for the simulation of compressible reacting flow. Part I. Accuracy and efficiency of algorithm, Journal of Computational Physics 272 (2014) 814 – 841.

[5] S. Paolucci, Z. J. Zikoski, T. Grenga, WAMR: An adaptive wavelet method for the simulation of compressible reacting flow. Part II. The parallel algorithm, Journal of Computational Physics 272 (2014) 842 – 864.

[6] T. Grenga, Numerical solutions of multi-dimensional compressible reactive flow using a parallel wavelet adaptive multiresolution method, Ph.D. thesis, University of Notre Dame, Notre Dame, IN 46556 (2015).

[7] S. R. Brill, T. Grenga, J. M. Powers, S. Paolucci, Automatic error estimation and verification using an adaptive wavelet method, 11th World Congress on Computational Mechanics (WCCM XI), 2014 (July 2014).

[8] D. Wirasaet, Numerical solutions of multidimensional partial differential equations using an adaptive wavelet method, Ph.D. thesis, University of Notre Dame, Notre Dame, IN 46556 (2008).

[9] H. Pitsch, N. Peters, A Consistent Flamelet Formulation for Non-Premixed Combustion Considering Differential Diffusion Effects, Combustion and Flame 114 (1) (1998) 26 – 40.

[10] S. S. Girimaji, On the modeling of scalar diffusion in isotropic turbulence, Physics of Fluids 4 (1992) 2529 – 2537.

[11] E. Petersen, R. K. Hanson, Reduced kinetics mechanisms for ram accelerator combustion, Journal of Propulsion and Power - J PROPUL POWER 15 (1999) 591–600 (07).

[12] M. Cismondi, J. Mollerup, Development and application of a three-parameter RK-PR equation of state, Fluid Phase Equilibria 232 (1) (2005) 74 – 89.

[13] M. O. M. Eric W. Lemmon, D. G. Friend, Thermophysical Properties of Fluid Systems, NIST Chemistry WebBook, NIST Standard Reference Database Number 69, National Institute of Standards and Technology, Gaithersburg MD, 20899, Eds. P.J. Linstrom and W.G. Mallard Edition (2019).